Title
SURFACE CHARACTERIZATIONOF SILICON NITRIDE AND SILICON CARBIDE POWDERS

Authors
Rahaman, M.N.
Boiteux, Y.
Jonghe, L.C. De

Publication Date
1985-10-01

Lawrence Berkeley Laboratory
UNIVERSITY OF CALIFORNIA

Materials & Molecular Research Division

Submitted to American Ceramic Society. Bulletin

SURFACE CHARACTERIZATION OF SILICON NITRIDE AND SILICON CARBIDE POWDERS

M.N. Rahaman, Y. Boiteux and L.C. De Jonghe

October 1985

Prepared for the U.S. Department of Energy under Contract DE-AC03-76SF00098

DISCLAIMER

SURFACE CHARACTERIZATION OF SILICON NITRIDE AND SILICON CARBIDE POWDERS

M. N. Rahaman*, Y. Boiteux* and L. C. De Jonghe*

Lawrence Berkeley Laboratory
University of California
Berkeley, California 94720

The nature and composition of the surfaces of silicon nitride and silicon carbide powders were investigated using high voltage and high resolution transmission electron microscopy (TEM), x-ray photoelectron spectroscopy (XPS), and secondary ion mass spectrometry (SIMS). An amorphous silica layer, ~ 5nm thick, present on the powder surfaces forms strong bridges between particles. Both XPS and SIMS show that oxygen is the major impurity on the powder surfaces but minor impurities such as chlorine, fluorine, carbon, iron and sodium are also revealed. The extent of the silica layer was reduced substantially by washing the powder in anhydrous hydrofluoric acid or by treatment in an argon/hydrogen gas mixture at 1300°C. The surface treatment in the gas mixture did not cause any further agglomeration of the powder.

Presented in part at the 87th Annual Meeting and Exposition, The American Ceramic Society, Cincinnati, OH, May 7, 1985 (Basic Science Division, Paper No. 98-B-85). Supported by the Division of Materials Sciences, Office of Basic Energy Sciences, U.S. Department of Energy, under Contract No., DE-AC03-76SF00098.

*Member, the American Ceramic Society.

I. INTRODUCTION

Silicon nitride and silicon carbide are currently used in a number of industrial applications and are also considered for high temperature, load bearing applications such as in heat engines. They are made by consolidating powders to form a green body, followed by sintering with or without applied pressure, to form a strong, dense component. It is being recognized that inhomogeneities, such as large pores, hard agglomerates, and density variations, present in the green body, may remain or may be enhanced during the sintering process. Increasing attention is therefore directed at processing methods which may result in a more homogeneous green microstructure. Colloidal processing methods are potentially more useful than dry pressing. [1,2] In colloidal processing, surface chemistry is of fundamental importance. Another area in the processing of silicon nitride and silicon carbide deserving much attention is connected with the composition of the grain boundary phases. In silicon carbide, for example, an oxygen content greater than ~ 0.5%, present as silica on the powder surface, hinders the sintering process and makes it difficult for near-theoretical density to be attained.[3,4] In silicon nitride, additives, such as Y_2O_3 and Al_2O_3, react with the SiO_2 on the powder surface to form a viscous phase at the sintering temperature. Uncertainties about the extent of the SiO_2 layer or any impurities added during milling of the powders may lead to phases which soften at relatively low tempratures.[5] It is therefore important to determine not only the extent of the silica layer but also manipulate it to the desired thickness. Various methods have been used for the removal of

surface silica from silicon nitride and silicon carbide powders. These involved washing the powder in aqueous NaOH or HF at room temperature [6,7] or vacuum treating [8,9] at 1300 - 1400°C. Washing the powder in aqueous solutions causes severe agglomeration on drying, and requires a subsequent grinding step. Contamination of the powder surface with fluorine in the aqueous HF treatment also results. Another method reported recently[10] uses boron trichloride gas or, more effectively, hydrogen fluoride. It is not known whether the gaseous HF treatment also causes contamination of the powder surfaces with fluorine. To increase the silica content of the powders SiO_2 may be added, the particle size of the powders may be reduced,[11] or the powder may be subjected to controlled oxidation.[12]

This paper deals first with the use of advanced techniques to characterize the surfaces of silicon nitride and silicon carbide powders, and second with the use of an argon/hydrogen gas mixture to remove surface silica from these powders. The gas treatment used to remove surface silica consisted of heating the powders at 1300°C in a flowing gas mixture of argon containing 5% hydrogen. For comparison, the powders were also treated in anhydrous hydrofluoric acid at room temperature. The surface characterization techniques used are high voltage and high-resolution transmission electron microscopy (TEM), x-ray photoelectron spectroscopy (XPS), and secondary ion mass spectrometry (SIMS). This is a first report in which emphasis is placed on experimental techniques, on the results that can be derived

for these powders, and on some of the complexities of the results. TEM is used to study the nature and extent of the surface features, including surface silica. XPS is used to determine the oxidation state of the elements on the surface in addition to their qualitative and quantitative analysis. SIMS is used for rapid identification of the elements on the surface and as a complementary technique to XPS. Auger electron spectroscopy was also attempted, but, because of the insulating nature of these powders., considerable charging of the sample was experienced.

II. EXPERIMENTAL

(i) Powders

Silicon nitride powders were obtained from three manufacturers: Starck* (denoted as Starck-SN), GTE+ (GTE-SN), and D.F. Goldsmith& (DFG-SN). These commercial powders were used because they were readily available from their manufacturers. A silicon carbide powder obtained from Norton company++ (Norton-SC) was also examined.

*LC 12, H.C. Starck, Inc., NY 10017

+SN 502, GTE Products Corp, Towanda, PA 18848

& 325 Mesh, D.F. Goldsmith Chemical and MetalCorp, Evanston, IL 60202

++Norton Company, Worcester, MA 01606

(ii) Transmission Electron Microscopy

All samples were prepared using the same dispersion method. A dilute dispersion (10^{-3}g per cm^3) of the powder in acetone was homogenized by an ultrasonic probe. Then, a few drops of the dispersion were deposited on a 3mm diameter copper grid, followed by evaporation of the solvent. This technique was used since it was unlikely to alter the powder surfaces.

High voltage microscopy was performed using a Kratos 1.5 MeV microscope while high resolution microscopy was performed using a Siemens 102 microscope.** Both microscopes are part of the National Center for Electron Microscopy, Lawrence Berkeley Laboratory, Berkeley, CA. Some micrographs were taken in the bright field mode, allowing only the transmitted beam through the smallest objective aperture. Lattice fringes were imaged using the standard technique, by recombining the transmitted beam with a strongly diffracted one through a larger aperture.

(iii) Secondary Ion Mass Spectrometry (SIMS)

The basic principle of SIMS is the ejection of atoms, ions and ion clusters from the surface of the sample by the impact of incident energetic ions.[13-16] The sputtered secondary ions are collected and mass analysed.

** Siemens Elmiscope 102, Siemens AG, Karlsruhe, Federal Republic of Germany.

A commercial instrument* was used for these studies. Samples were prepared by drying the powder overnight in a vacuum furnace operating at 150°C, followed by pressing it into small pellets. The surfaces of the pellets were rubbed on filter paper to remove any metallic contamination from the die. An argon ion beam, of energy 4 keV, was employed as the sputtering beam.

(iv) X-ray Photoelectron Spectroscopy (XPS)

Surface analysis by XPS involves the irradiation of a sample *in vacuo* (10^{-9}-10^{-10} atm) with monoenergetic soft x-rays and the energy analysis of the emitted photoelectrons. [17-19] Since the escape depth of the photoelectrons is small, this technique is selective to a surface depth of a few nanometers.

The x-ray photoelectron spectrometer used is a Physical Electronics 548 ESCA/Auger system.* The output from the photoelectron detector is amplified and analysed, and then the data are transferred to a micro-computer. The XPS data analysis program is a simple, non-iterative curve fitting routine which uses a Gaussian line-shape and an S- shaped background. This data collection and analysis system is described in detail elesewhere.[20] The x-rays used to bombard the sample were monochromatic MgK_{α} rays with an energy of 1253.6 eV.

*Perkin-Elmer Corporation, Physical Electronics Division, Minnesota 55344

Powder samples were dried overnight in a vacuum furnace operating at 150°C. Two different methods were used for mounting the powders for XPS analysis. In the indium foil method, powder was pressed between two pieces of indium foil. The pieces were then separated, and one of them was mounted for analysis. The success of this method was variable, since it was difficult to achieve a uniform coverage of powder on the foil. Any uncovered areas would make a strong contribution to the signals from the indium foil itself. In the other method, a strip of polymer-based adhesive tape was used, and a small amount of powder dusted on to achieve a nearly uniform coverage. This method proved to be more reproducible and was used here.

(V) Manipulation of Surface Silica on the Powders.

To control and reduce the silica layer on the powders, two different surface treatment methods were used. In one method, a known mass of powder was treated in a flowing gas mixture* ($100 cm^3\ min^{-1}$) of argon/5% hydrogen at 1300°C for a known period of time. In the other method, the powder was leached in anhydrous hydrofluoric acid** for a known time, then dried and ground in an agate mortar and pestle to break up the agglomerates. The treated powders were stored in a vacuum dessicator prior to analysis. Oxygen contents were measured by neutron activation analysis#.

* Pacific Oxygen Company, Oakland, CA 94607
** Mallinckrodt Inc., Paris, Kentucky 40361
# IRT, P.O. Box 85317, San Diego, CA 92138-5317

III. RESULTS AND DISCUSSION

(i) Transmission Electron Microscopy (TEM)

Figure 1 shows a high voltage electron micrograph of DFG silicon nitride (DFG-SN). Closer examination of the contact area between the particle shows that they are connected by a strong amorphous bridge, presumably silica. Figures 2 and 3 show high resolution electron micrographs of Starck silicon nitride (Starck-SN) and Norton silicon carbide (Norton-SC), respectively. The amorphous silica layer on the powders is clearly revealed, and is and ~3-5 nm thick.

Since the agglomerates can be bonded by strong silica bridges, the main methods of breaking them up may be (a) mechanically, by milling, for example, and (b) chemically, by reducing the silica. The mechanical method suffers from the disadvantage that impurities are introduced into the powder. These impurities, such as metal oxides and additional silica are also difficult to control during milling or grinding. The chemical method may be a much cleaner method if the reducing agent and the unwanted reaction products are removed in the gaseous phase.

(ii) Secondary Ion Mass Spectrometry (SIMS)

Figure 4 shows the positive and negative secondary ion mass spectra of GTE silicon nitride (GTE-SN). The secondary ion signal was produced from a thickness of ~1nm below the surface of the sample. It is seen that the major impurity is oxygen, but there are also small

amounts of Cl, F and Na. Traces of Li, K, Cu, and Fe were also detected. Information about the chemical environment and quantitative estimates of these elements cannot be readily obtained by this technique. In addition, and inherent characteristic of SIMS is that it destroys the surface that it analyses. However, this technique proved to be quick and extremely sensitive for the detection of the elements on the surface.

(iii) X-ray Photoelectron Spectroscopy (XPS)

An x-ray photoelectron spectrum of GTE-SN, produced by scanning over a wide energy range (0-1 keV), is shown in figure 5. The elements detected agree with the results obtained using SIMS. The real advantage of XPS, however, is that scanning can be performed over a narrow energy range to obtain information on the chemical environment and semi-quantitative or quantitative estimates of the surface element concentration.

Figure 6 shows an example of a scan over a narrow energy range (517-542eV) to detect photoelectrons emitted from the 1δ energy level of oxygen, O(1δ). The best fit to the results is obtained by using two peaks, the larger occurring at 535.4 eV and the smaller at 532.5eV. The ratio of the peak areas is 1:12. The peak positions have to be corrected because of static charging of the sample. Experiments have shown that charging results in an increase (2-3 eV) in the peak position compared with standard data.[21] However, this increase is constant, to within 0.2 eV, over the entire energy range for the

duration of the analysis of a sample (~8 hours). The adventitious carbon 1s peak, arising from traces of hydrocarbons in the spectrometer, was used as a reference for evaluating the peak positions. The C(1s) peak was observed at the beginning and at the end of the analysis and the peak shift due to charging was taken as the average value minus the value of 284.6 eV, obtained from standard data.[21] For a nearly uniform thickness of sample, charging was found to cause approximately the same shift for all the elemental spectra. The corrected peak positions of figure 6 are then 532.6 and 529.7 eV. The peak at 532.6 eV corresponds to oxygen bonded to silicon in SiO_2, while that at 529.7 eV arises from oxygen in a metalic oxide (such as iron oxide) or from adsorbed oxide contamination.

For comparison, the O(1s) line for Starck-SN is shown in figure 7. The largest peak at 532.5 eV (after correction for static charging) corresponds to oxygen in SiO_2. The best fit of the data also involves two smaller peaks, one at 530.0 eV, arising from iron oxide, Fe_2O_3, and the other at 527.5 eV due to the presence of other, unidentified impurities. It is quite clear, however, that this Starck-SN contains relatively more of these minor oxide impurities than the GTE-SN.

Figure 8 shows a detailed spectrum of the fluorine 1s line detected in GTE-SN. The corrected peak positions are 687.6 eV and 683.8 eV. The higher binding energy peak arises from F bonded to Si, while the peak at the lower binding energy arises from an alkali metal fluoride,

possibly NaF. The atomic concentration (C_x) of any element X was determend from the expression

$$C_x = \frac{I_x/S_x}{\Sigma_i \; I_i/S_i}$$

where I_x is the relative peak area of the line spectrum for element X and S_x is the calculated atomic sensitivity factor.[21] The atomic concentrations of fluorine in GTE-SN and Starck-SN, 0.04 and 0.07 respectively, are sufficiently high to affect the processing behaviour of these powders.

Figures 9(a) and 9(b) compares the silicon 2*p* lines in GTE-SN and Norton-SC, respectively. For Norton-SC, the spectrum may be resolved into two peaks: Si in silicon carbide (peak position at 100.2 eV) and Si in silica (102.8 eV). For GTE-SN, the best fit of the spectrum consists of one peak (peak position 102.2 eV) having the same width as those for the Norton-SC spectrum. The peak position is noticeably lower than the value of 103-103.5 eV obtained from standard data.[21] It appears that the XPS technique samples depths that include regions below the native silica layer for both Norton-SC and GTE-SN. The reason for this single peak spectrum in GTE-SN cannot be convincingly explained at the present time.

The positions of the line spectra after correction for static surface charging are shown in Table I for GTE-SN. Included in this table are the most likely interpretation of the chemical compounds associated with the elements detected. Table I also shows the

calculated quantities of these elements present in the surface thickness analysed by XPS.

Table I: Line Positions, Chemical Compounds and Elemental Concentrations (C_x) derived using XPS for GTE Silicon Nitride

Line Spectrum	Position (eV)	Chemical Compound	Concentration (C_x)
Si (2p)	102.2	SiO_2, Si_3N_4	0.38
O (1s)	532.6	SiO_2	0.16
O (1s)	529.7	Fe_2O_3, adsorbed impurities	0.01
N (1s)	397.8	Si_3N_4	0.38
F (1s)	687.6	Fluorinated Si	0.03
F (1s)	683.8	LiF, NaF	0.01
Cl (2s)	200.8	Chlorinated Si	0.01
C (1s)	284.6	Free carbon and Hydrocarbons	0.02

Using the calculated elemental concentrations in Table I, the best specification of the surface layer analysed by XPS is SiO_2 + 1.2 Si_3N_4 + minor quantities of fluorinated and chlorinated silicon compounds and oxygen compounds. The exact composition of these minor compounds is difficult to derive. Since the electron micrographs of figures 2 and 3 show that the silica layer is fairly uniform in thickness (3-5nm), it appears that a (total) surface layer with a thickness of 5-10 nm is

sampled for this powder. Future work will include grazing angle XPS to enhance the surface sensitvity.

(iv) Surface Silica Manipulation

Table II shows the oxygen contents (in weight percent) of GTE-SN, Starck-SN and Norton-SC, 'as received' from the manufacturers (denoted AR) and following surface treatments in anhydrous hydrofluoric acid (denoted HF) and in Ar/5%H_2 at 1300°C (denoted GAS). The HF treatment and the gas treatment lasted for 6 hrs and 12 hrs respectively. The results for the 'as received' powders and HF treated powders were determined by neutron activation analysis. Those for the gas treated powders were determined using XPS, by comparing the oxygen concentration with the value obtained for the 'as received' powder.

Figure 10 shows a high resolution TEM micrograph of Starck-SN that has undergone HF treatment. It is seen that the silica layer is much reduced compared with that of figure 2, and is ~2-3 nm thick.

Table II: Oxygen contents (in weight percent) of powders as received (AR), and following treatments in HF and a mixed gas of Ar/5%H_2 at 1300°C.

Powders	Oxygen Content (wt.%)		
	AR	HF	GAS
GTE-SN	1.1	0.9	-----
Starck-SN	4.1	2.1	1.4
Norton-SC	3.1	2.0	1.2

Both methods are effective in reducing the oxygen content of the powders, as seen from Table II. However, in case of the HF treatment, the resulting powder is highly agglomerated. Some of these agglomerates can be quite difficult to break up. Also, there is appreciable fluorine contamination, which can alter the subsequent processing behaviour of the powder. In contrast, the gas treatment does not cause any noticeable increase in agglomeration.

IV CONCLUSIONS

The techniques used in this work, namely high resolution and high voltage TEM, XPS and SIMS have proved to be useful for characterizing the surface structure and surface chemistry of silicon nitride and silicon carbide powders. The XPS and SIMS techniques are best used in conjunction and do not suffer from excessive static surface charging, as is the case in Auger spectroscopy of these predominantly insulating powders.

The powders used are shown to have a native silica layer, 5nm thick, which may form strong bridges between individual particles. Oxygen from this layer is the major surface impurity but smaller quantities of F, Cl, C, Fe, Al, Ca and Na have been readily detected. The presence of these impurities can affect the processing behaviour, and may be detrimental to high temperature properties if they are not controlled.

Treatment of the powders in a gas mixture of Ar/5%H_2 at 1300°C is effective in reducing the oxygen content of the powders. This method does not cause agglomeration nor does it introduce additional impurities into the powder.

Acknowledgments: The authors wish to thank K. Gaugler and B. Beard for instruction and help in using the SIMS and XPS equipment, and the National Center for Electron Microscopy for use of the electron microscopes.

REFERENCES

1. J. Th. G. Overbeek "Recent Development in the Understanding of Colloid Stability" J. Colloid Interface Sci. 58 2 408-22 (1977).

2. I. A. Aksay, F. F. Lange and B. I. Davis "Uniformity of Al_2O_3-ZrO_2 by Colloidal Filtration" J. Am. Ceram. Soc. 66 10 C190-92 (1983).

3. S. Prochazka "Sintered Dense Silicon Carbide" U.S. Pat. 4 004 934 January 1977.

4. J. A. Coppola, H. A. Lawler and C. H. Mc Murty "Silicon Carbide Powder Compositions" U. S. Pat. 4 123 486 October 1978.

5. F. F. Lange "Fabrication and Properties of Dense Polyphase Silicon Nitride" Ceramic Bulletin 62 12 1369-74 (1983).

6. S. Prochazka and R. M. Scanlan "Effect of Boron and Carbon on Sintering of SiC" J. Am. Ceram. Soc., 58 1-2 72 (1975).

7. W. Bocker and H. Hausner "The Influence of Boron and Carbon on Additions on the Microstructure of Sintered Alpha SiC' Powder Metall. Int., 10 3 87 (1978).

8. T. R. Wright and D. E. Niesz "Improved Toughness of Refractory compounds" Tech. Rep. NASA CR-134690, October 1974.

9. C. Greskovitch, S. Prochazka and J. H. Rosolowski "Basic Research on Technology Development for Sintered Ceramics" Tech. Rep. No. AFML TR-76-179, General Electric Co., NY, 1976.

10. J. Brynestad, C. E. Bamberger, D. E. Heatherly and J. F. Land "Removal of Oxide Contamination from Silicon Carbide Powders" J. Am. Ceram. Soc., 67 9 C184-85 (1984).

11. S. Prochazka and C. Greskovich "Development of a Sintering Process for High Performance Si_3N_4" Tech. Rep. AMMRC TR-78-32, July 1978.

12. C. Greskovich and J. A. Palm "Controlling the Oxygen Content of Si_3N_4 Powders" Ceramic Bulletin 59 11 1155-56 (1980).

13. G. A. Somorjai and M. Salmeron "Surface Characterization of Ceramic Materials" in Ceramic Microstructures '76, R. M. Fulrath and J. A. Pask (ed.), Westview Press, Colorado, pp. 101-128, 1976.

14. H. W. Werner "The Use of Secondary Ion Mass Spectrometry in Surface Analysis" Surf. Sci., 47, 301 (1975).

15. A. Benninghoven "Developments in Secondary Ion Mass Spectrometry and Applications to Surface Science" Surf. Sci., 53, 596 (1975).

16. J. A. Mc Hugh "Secondary Ion Mass Spectrometry ", in Methods of Surface Analysis, A. W. Czanderna (ed.), Elsevier, Amsterdam, 1975.

17. K. Siegbahn "ESCA-Atomic, Molecular and Solid State Structure Studied by Means of Electron Spectroscopy" Almquist and Wiksells, Uppsala, 1967.

18. K. Siegbahn "Electron Spectroscopy-An Outlook", J. Electron Spectros. and Related Phenomena, 5 3-97, Nov./Dec. 1974.

19. W. M. Riggs and M. J. Parker "Surface Analysis by X-ray Photoelectron Spectroscopy" in Methods of Surface Analysis, A. W. Czanderna (ed.) Elsevier, Amsterdam, 1975.

20. B. C. Beard, D. Dahlgren and P. N. Ross "Microcomputer-Multichannel Analyser Data System for Foreground-Background Data Collection and Analysis", J. Vac. Sci. Tech. (A)., Sept./Oct. 1975, to be published.

21. C. D. Wagner, W. M. Riggs, L. E. Davis, J. F. Moulder and G. E. Muilenberg (ed.), "Handbook of X-ray Photoelectron Spectroscopy", Perkin-Elmer Corp. MN 55344 (1978).

LIST OF FIGURES

Figure 1. High voltage electron micrograph of DFG silicon nitride, showing particles connected by strong, amorphous silica bridges.

Figure 2. High resolution electron micrograph of Starck silicon nitride showing an amorphous, fairly uniform silica layer ~ 3-5 nm thick.

Figure 3. High resolution electron micrograph of Norton silicon carbide, showing the native silica layer.

Figure 4. Positive and negative secondary ion mass spectra of GTE silicon nitride.

Figure 5. X-ray photoelectron spectrum of GTE silicon nitride obtained from a survey scan between 0 and 1 keV.

Figure 6. The oxygen 1s line spectrum in GTE silicon nitride obtained by X-ray photoelectron spectroscopy.

Figure 7. The oxygen 1s line spectrum in Starck silicon nitride. Minor differences from the spectrum in Figure 6 can be clearly seen.

Figure 8. The fluorine 1s line spectrum in GTE silicon nitride.

Figure 9. The silicon 2p line spectra in (a) GTE silicon nitride and (b) Norton silicon carbide.

Figure 10. High resolution electron micrograph of Starck silicon nitride that has been treated in anhydrous hydrofluoric acid. A much reduced silica layer, compared to Figure 2, of ~ 2-3 nm, is revealed.

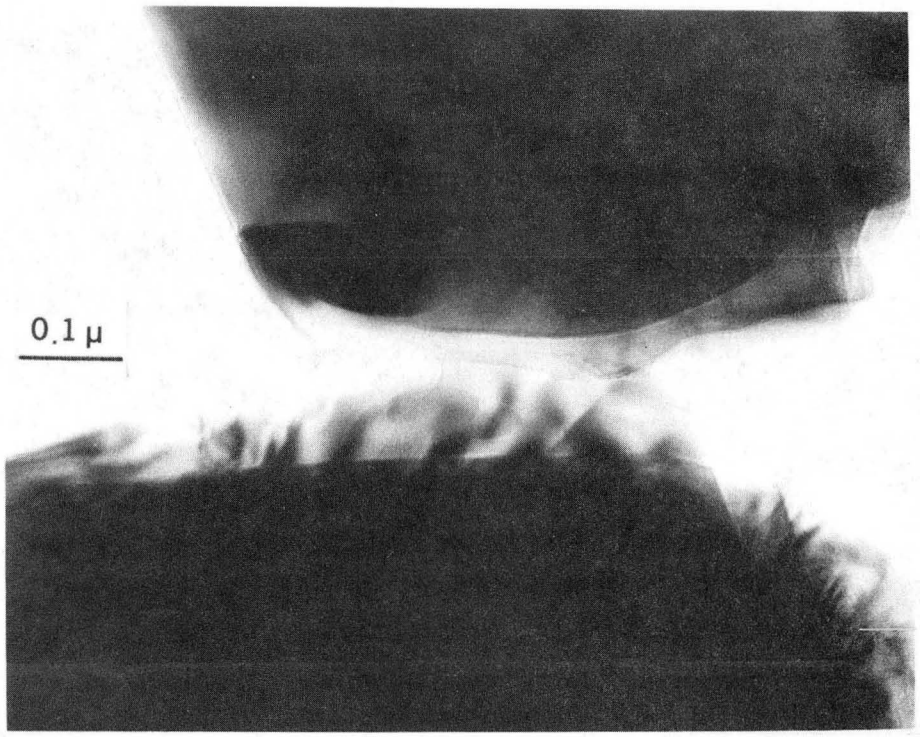

XBB 850-8116

Fig. 1

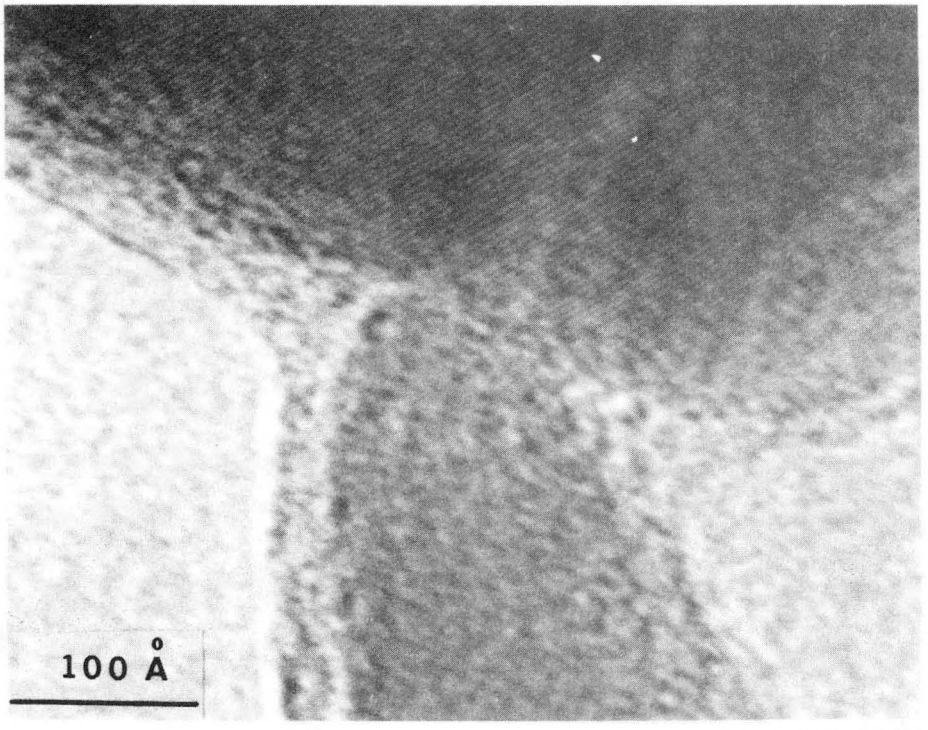

XBB 850-8115

Fig. 2

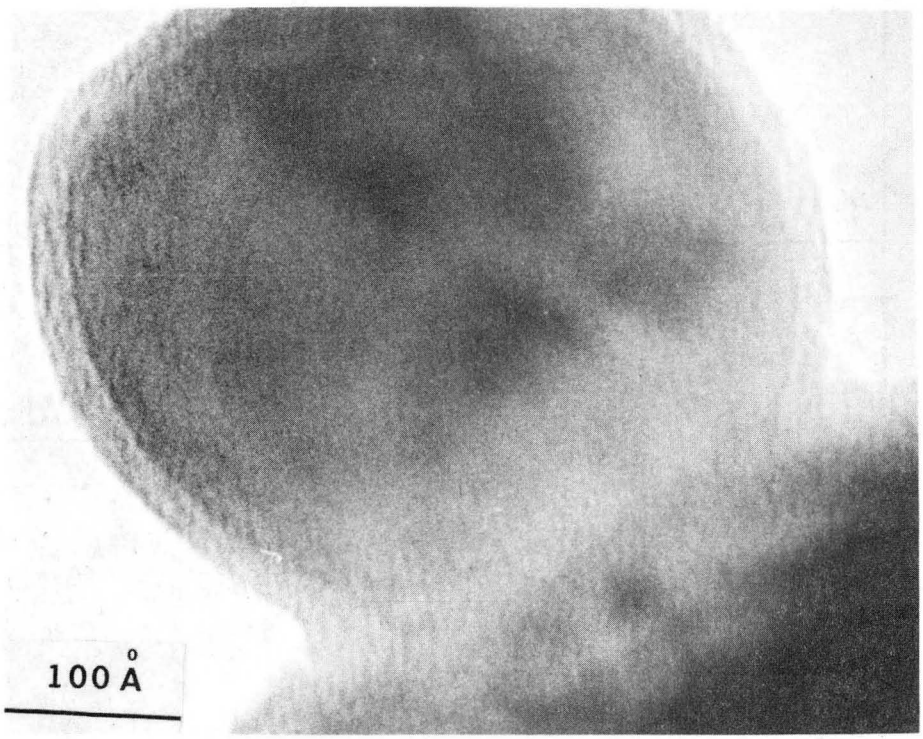

XBB 850-8114

Fig. 3

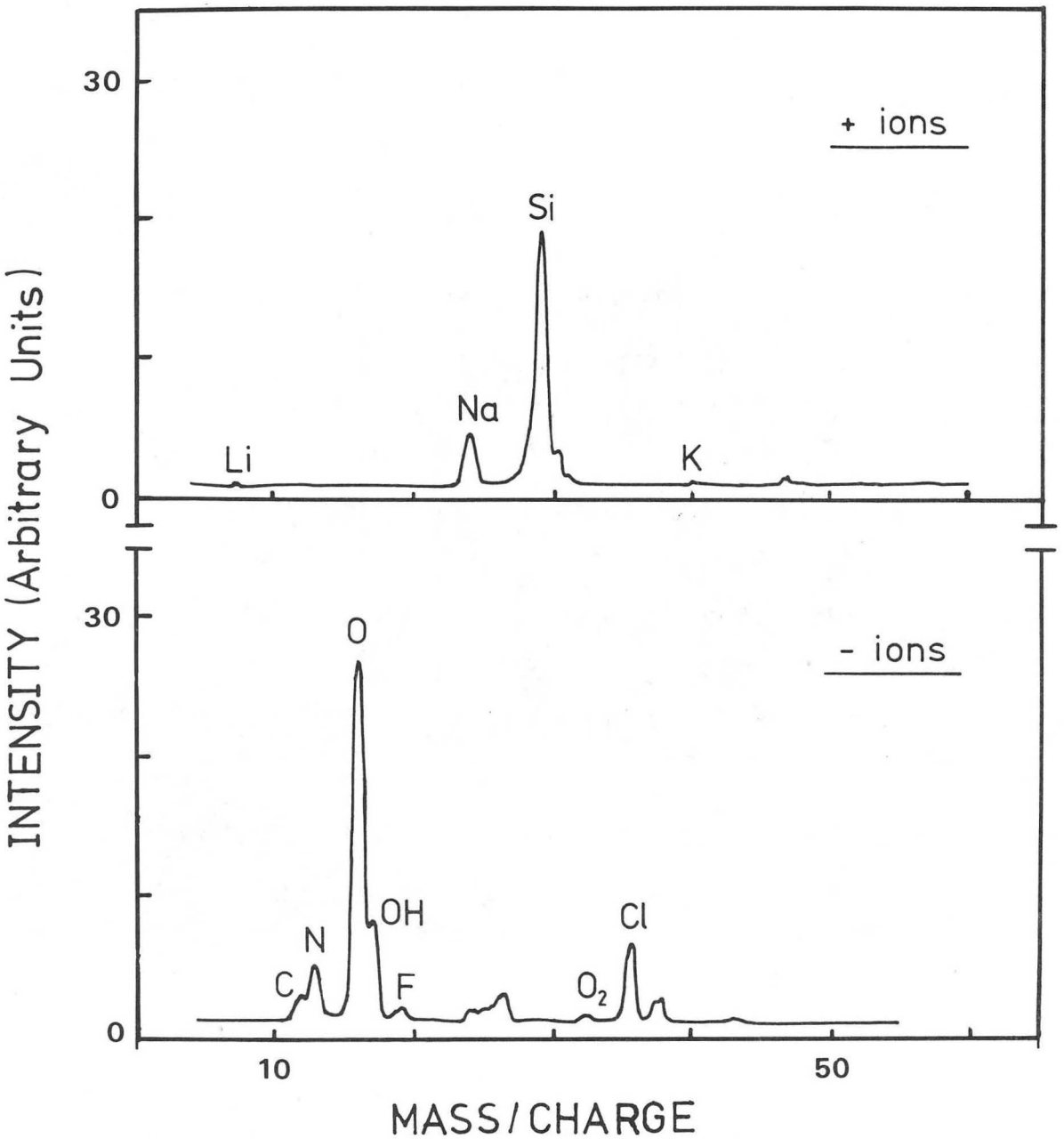

Fig. 4

XBL 848-3430

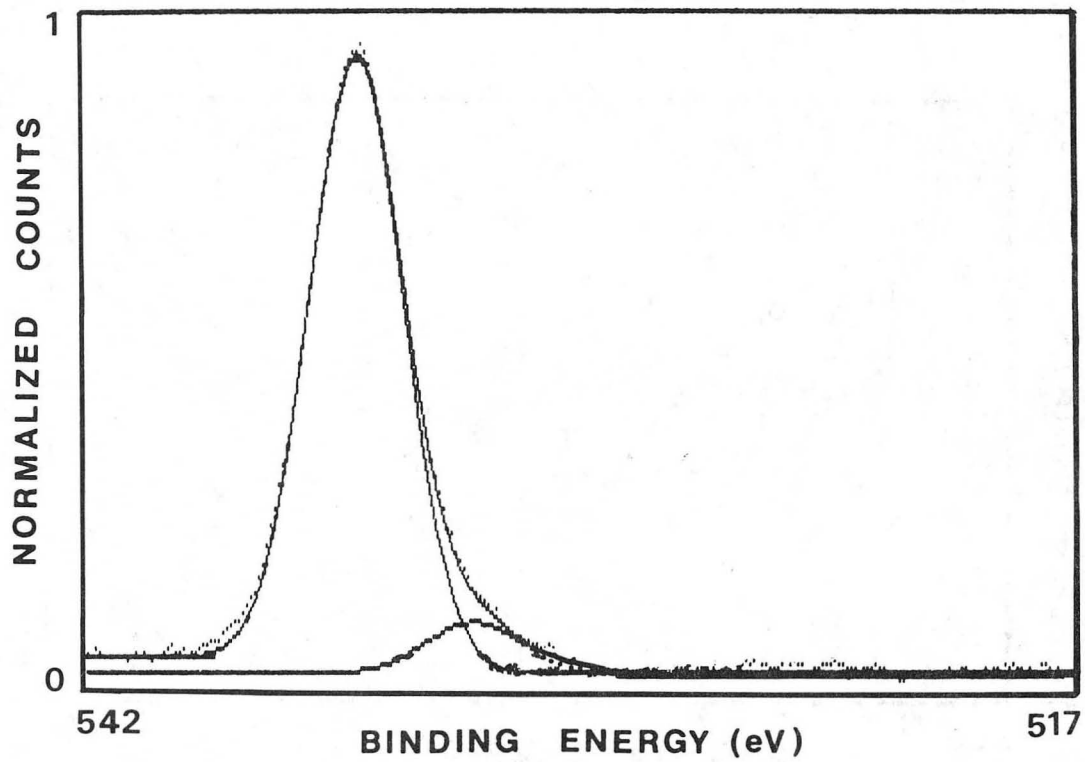

XBL 859-4103

Fig. 5

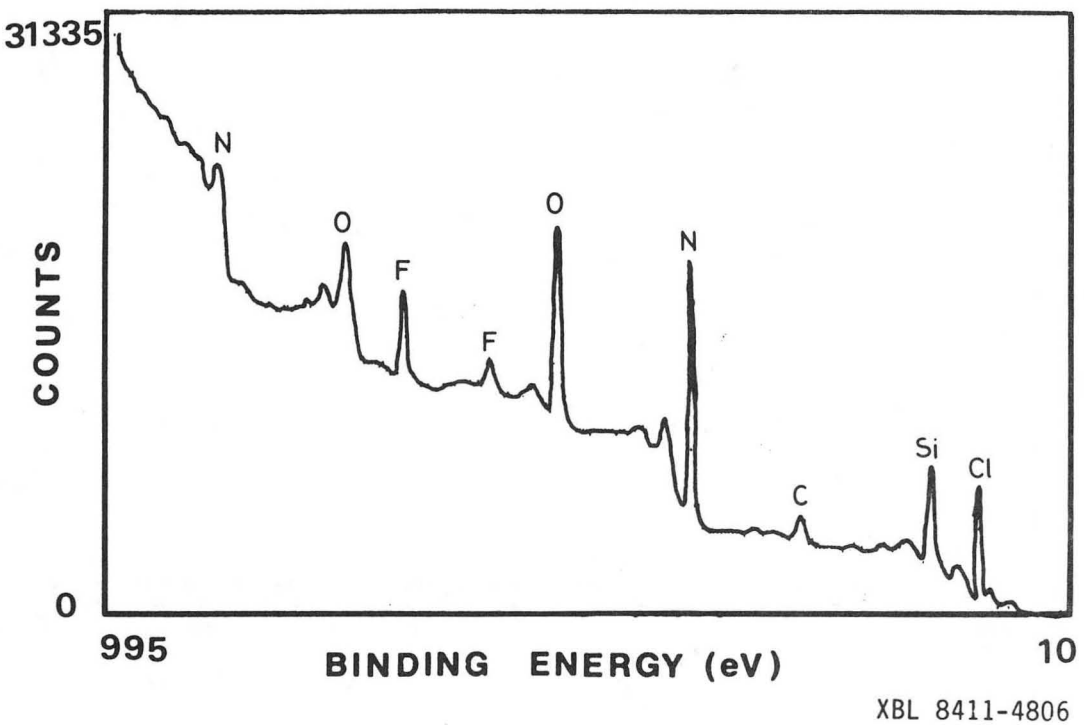
31335
COUNTS
0
N
O
F
F
O
N
C
Si
Cl
995
BINDING ENERGY (eV)
10
XBL 8411-4806

Fig. 6

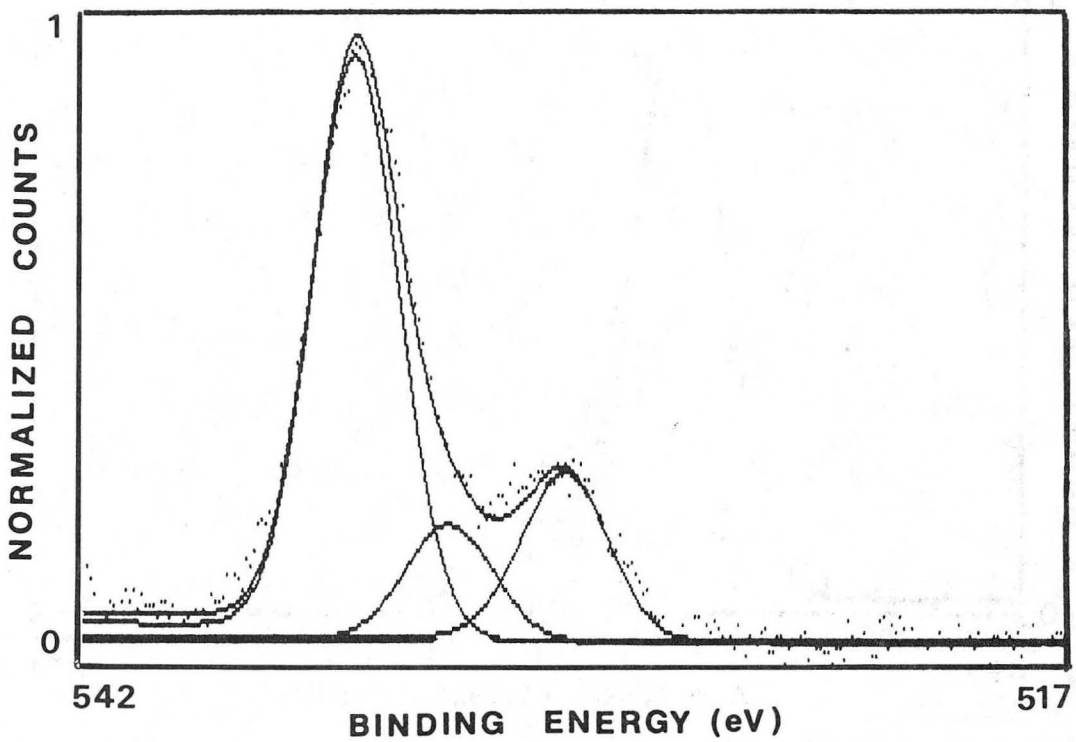

XBL 859-4105

Fig. 7

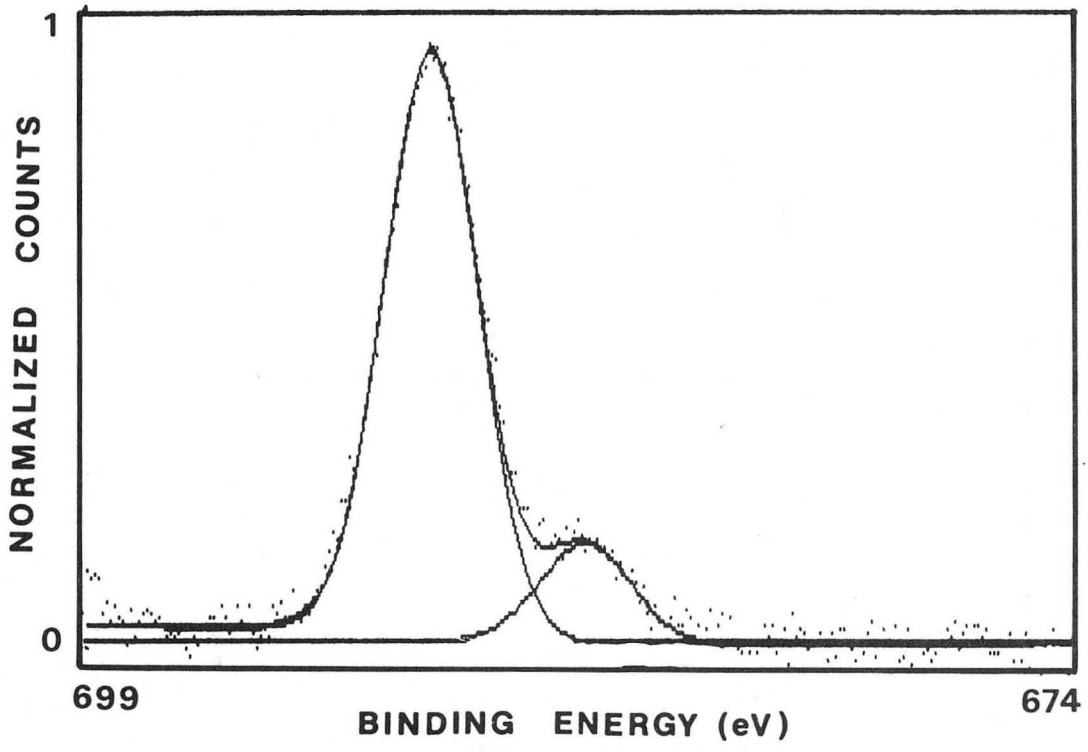

XBL 859-4104

Fig. 8

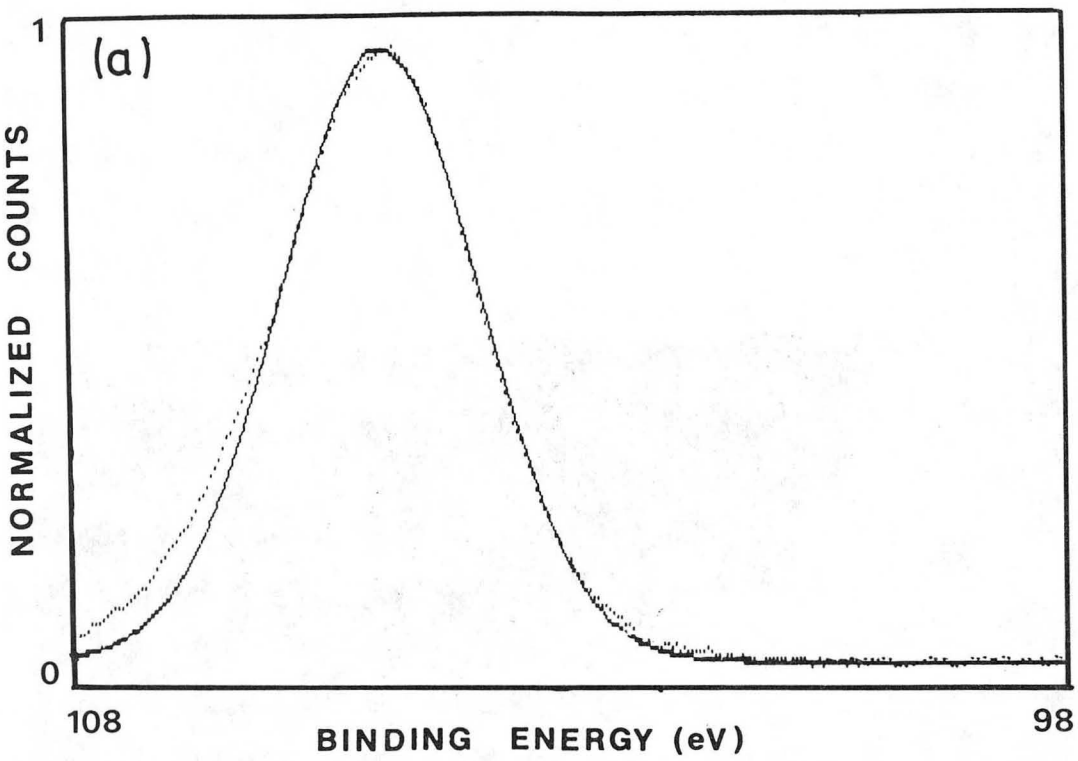

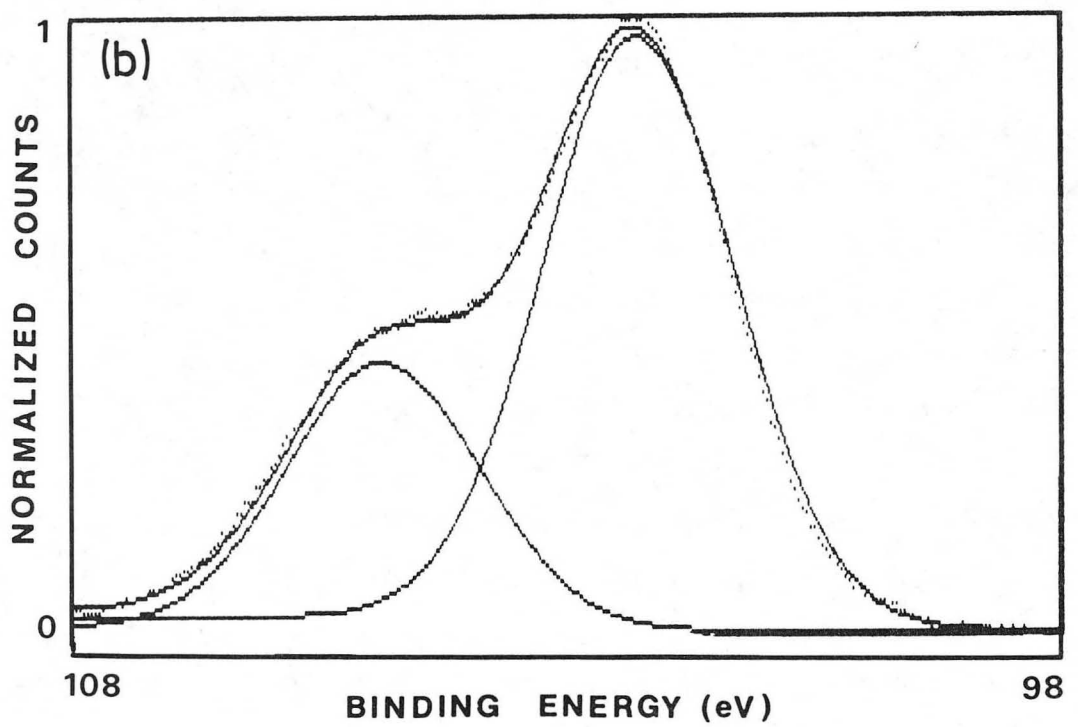

XBL 859-4106

Fig. 9

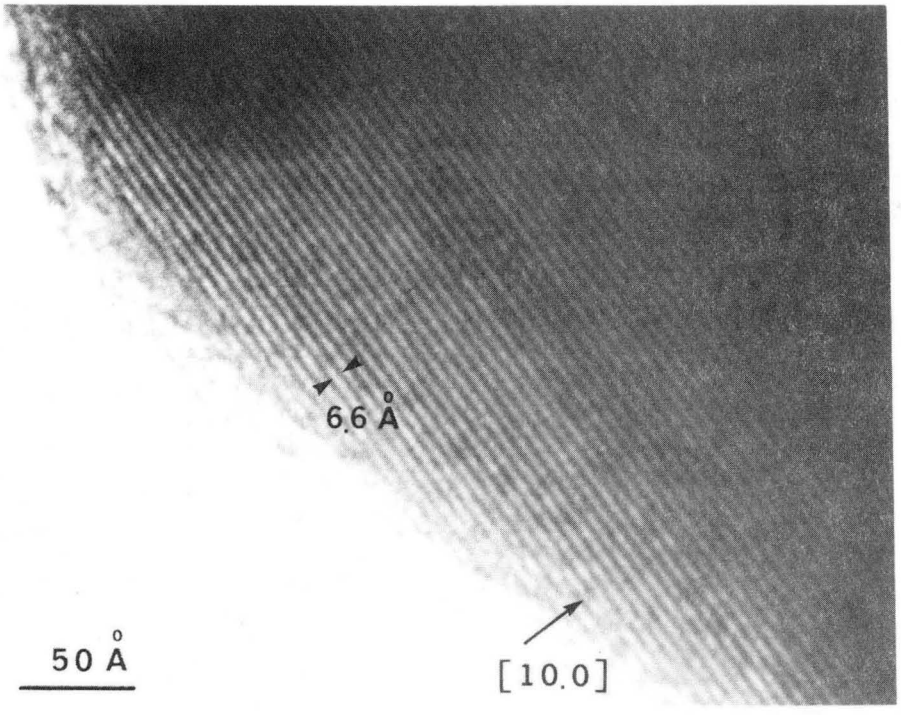

Fig. 10

LAWRENCE BERKELEY LABORATORY
TECHNICAL INFORMATION DEPARTMENT
UNIVERSITY OF CALIFORNIA
BERKELEY, CALIFORNIA 94720